Materials Research. 2017; 20(4): 1057-1062
DOI: http://dx.doi.org/10.1590/1980-5373-MR-2016-0894

Phase Equilibria in the Tl_5Te_3-Tl_9BiTe_6-Tl_9TmTe_6 Section of the Tl-Bi-Tm-Te Quaternary System

Samira Zakir Imamaliyeva[a]*, Mehdiyeva Ilaha Firudin[a], Vagif Akber Gasymov[a], Mahammad Baba Babanly[a]

[a] *Institute of Catalysis and Inorganic Chemistry named after acad.M.Nagiyev, ANAS H.Javid ave., 113, Az-1143, Baku, Azerbaijan*

Received: November 30, 2016; Revised: April 14, 2017; Accepted: May 21, 2017

Phase relations in the Tl_5Te_3-Tl_9BiTe_6-Tl_9TmTe_6 section of the Tl-Bi-Tm-Te quaternary system were studied by differential thermal analysis, powder X-ray diffraction technique and microhardness measurements applied to equilibria alloys. Some isopleth sections and isothermal section at 760 K, as well as projections of the liquidus and solidus surfaces, were constructed. The system is characterized by formation of continuous series of solid solutions at the solidus temperatures and below. Solid solutions are crystallized in the tetragonal Tl_5Te_3 structure type.

Keywords: *thallium-thulium tellurides, thallium-bismuth tellurides, phase relations, projections of the liquidus and solidus, solid solutions, crystal structure*

1. Introduction

Due to their important properties, chalcogenides based materials find applications in a range of devices such as optoelectronic and memory devices, ion-selective sensors, modern day solar cells, and thermoelectric energy conversion[1,2]. In recent years, a number of studies are devoted to the investigation of interactions of heavy metals chalcogenides with rare-earth elements[3-7].

Thallium subtelluride, Tl_5Te_3, because of features of crystal structure (Sp.gr.I4/mcm, a = 8.930; c = 12.598 Å)[8] has a number of ternary derivatives such as of $Tl_4A^{IV}Te_3$ and $Tl_9B^{V}Te_6$ (A^{IV}-Sn, Pb; B^{V}-Sb, Bi)[9-11].

Pointed compounds show a good thermoelectric performance, whereas Tl_9BiTe_6 exhibits the highest ZT value[2,12]. Furthermore, authors[13] found the Dirac-like surface states in the $[Tl_4]TlTe_3$ (Tl_5Te_3) and its non-superconducting tin-doped derivative $[Tl_4](Tl_{1-x}Sn_x)Te_3$.

Earlier we presented some new thallium lanthanide tellurides of Tl_9LnTe_6-type (Ln-Ce, Nd, Sm, Gd, Tm, Tb), which are also ternary substitution variant of Tl_5Te_3[14-16]. As it was shown[16,17], ytterbium does not form the compound of pointed type. Later, the crystal structure, magnetic and thermoelectric properties for a number of Tl_9LnTe_6-type compounds were determined by authors[18-20].

Doping is an effective way for improve the thermoelectric properties, because incorporation of heavy atoms into crystal lattice may significantly reduce the lattice contribution to the total thermal conductivity, which leads to an increase of the thermoelectric performance[21]. At this aim, we have presented the results of phase equilibria investigations of a number of systems including Tl_5Te_3 compound or its structural analogues[22-24]. We found that these systems are characterized by the formation of continuous series of solid solutions.

The present paper is aimed to investigate phase equilibria in the Tl_5Te_3-Tl_9BiTe_6-Tl_9TmTe_6 section of the Tl-Bi-Tm-Te quaternary system.

Starting compounds Tl_5Te_3 and Tl_9BiTe_6 melt congruently at 723 K[25] and 830 K[10] while Tl_9TmTe_6 melts with decomposition by the peritectic reaction at 745 K[26]. The crystal lattice parameters of Tl_9TmTe_6 and Tl_9BiTe_6 are following: a=8.9095, c=12.7412 Å, z=2; a = 8.855, c = 13.048 Å, z=2[26,27].

2. Experimental

2.1. Materials and syntheses

The following reagents were used as starting components: thallium (granules, 99.999 %), bismuth (granules, 99.999 %), thulium (powder, 99.9%), and tellurium (broken ingots 99.999 %).

The reagents were weighed according to the compositions and put into silica tubes of about 20 cm in length. Then the ampoules were sealed under a vacuum of 10^{-2} Pa. The samples, 1 gram each, were prepared by melting of the reagents in evacuated quartz ampoules in one zone electric furnace at the 30-50^0 above the melting point of the compounds followed by cooling in the switched-off furnace.

In the case of Tl_9TmTe_6, the ampoule was graphitized using pyrolysis of acetone in order to prevent the reaction of thulium with quartz. Taking into account the results of the[26], the intermediate ingot of Tl_9TmTe_6 was powdered in an agate mortar, pressed into a pellet and annealed at 700 K within ~700 h.

* e-mail: samira9597a@gmail.com

The purity of the synthesized starting compounds was checked by the differential thermal analysis (DTA) and X-ray diffraction (XRD).

Only one thermal effect was observed for Tl_9BiTe_6 (830 K) and Tl_5Te_3 (723 K), and two peaks for Tl_9TmTe_6 which are relevant to the peritectic reaction at 745 K and its liquidus at 1123 K. These data agree with the literature data[10,25,26].

XRD confirmed that the synthesized Tl_5Te_3, Tl_9BiTe_6, and Tl_9TmTe_6 compounds were phase-pure. Their powder XRD patterns were indexed using Topas V3.0 software. Obtained unit cell parameters were practically equal to those given in[8,26,27] (Table 1).

Previously synthesized binary and ternary compounds were used to synthesize the alloys of the Tl_5Te_3-Tl_9BiTe_6-Tl_9TmTe_6 system. Taking into account the results of previous studies that an equilibrium state could not be obtained even after the long-time (1000 h.) annealing[22,26], after synthesis the samples containing >60% Tl_9TmTe_6 were powdered, mixed, pressed into pellets and annealed at 700 K during ~ 800 h in order to complete the homogenization.

2.2. Methods

All alloys were studied by using differential thermal analysis, X-ray diffraction method and microhardness measurements.

DTA was performed using a NETZSCH 404 F1 Pegasus differential scanning calorimeter within room temperature and ~1400 K at a heating rate of 10 $K \cdot min^{-1}$ and accuracy about ±2 K. X-ray examination of powdered specimen was carried using a Bruker D8 diffractometer utilizing CuK_α radiation within $2\theta = 10 \div 70°$. The unit cell parameters of intermediate alloys were calculated by indexing of powder patterns using Topas V3.0 software. An accuracy of the crystal lattice parameters is shown in parentheses (Table 1).

Microhardness measurements were done with a microhardness tester PMT-3, the typical loading being 20 g and accuracy about 20 MPa.

3. Results and discussion

The Tl_5Te_3-Tl_9BiTe_6-Tl_9TmTe_6 section of the Tl-Bi-Tm-Te system was constructed based on obtained experimental results and literature data on boundary systems[10,26] (Figures 1-5).

Tl_9TmTe_6 melts with decomposition and loses the properties of the component of the system above the temperature of the peritectic reaction. Therefore, this compound inverted commas on the axes of the phase diagrams (Figures).

The results of DTA and microhardness measurements for alloys of boundary systems, as well as the parameters of the crystal lattices for some intermediate alloys, are given in the Table 1. Based on these data, T-x diagrams and the composition dependencies of corresponding properties are constructed.

$2Tl_5Te_3$-Tl_9TmTe_6 and Tl_9BiTe_6-Tl_9TmTe_6 systems. As can be seen (Figures 1, 2), these systems are characterized by the formation of continuous solid solutions (δ) with Tl_5Te_3-structure. However, they are non-quasi-binary sections of the Tl–Tm–Te ternary and Tl-Bi-Tm-Te quaternary systems due to peritectic melting of Tl_9TmTe_6 compound. This leads to crystallization infusible X phase in a wide composition range and formation L+X two-phase and L+X+δ three-phase

Table 1. Dependence of the properties of the alloys annealed at the 700 K (800 h) on the composition for the Tl_5Te_3- Tl_9TmTe_6 and Tl_9BiTe_6-Tl_9TmTe_6 sections of the Tl-Bi-Tm-Te quaternary system

Solid phase compositions	Thermal effects, K	Microhardness, MPa	Parameters of tetragonal lattice, Å	
			a	*c*
Tl_5Te_3	723	1130	8.9292(3)	12.5995(6)
$Tl_{9.9}Tm_{0.1}Te_6$	725-728	-	-	-
$Tl_{9.8}Tm_{0.2}Te_6$	726-730	1200	8.9259(4)	12.6266(11)
$Tl_{9.6}Tm_{0.4}Te_6$	730-735	1240	8.9218(5)	12.6553(12)
$Tl_{9.5}Tm_{0.5}Te_6$	732-737	-	-	-
$Tl_{9.4}Tm_{0.6}Te_6$	734-739	1260	8.9177(6)	12.6839(11)
$Tl_{9.2}Tm_{0.8}Te_6$	738-743; 1040	1240	8.9135(5)	12.7126(11)
$Tl_{9.1}Tm_{0.9}Te_6$	741-744; 1095	-	-	-
Tl_9TmTe_6	745; 1123	1210	8.9095(4)	12.7412(8)
$Tl_9Bi_{0.1}Tm_{0.9}Te_6$	750-770; 1100	-	-	-
$Tl_9Bi_{0.2}Tm_{0.8}Te_6$	755-788; 1050	1290	8.8981(4)	12.8022(11)
$Tl_9Bi_{0.4}Tm_{0.6}Te_6$	770-800	1260	8.8872(5)	12.8641(12)
$Tl_9Bi_{0.5}Tm_{0.5}Te_6$	775-805	-	-	-
$Tl_9Bi_{0.6}Tm_{0.4}Te_6$	777-810	1200	8.8761(5)	12.9263(10)
$Tl_9Bi_{0.8}Tm_{0.2}Te_6$	800-820	1120	8.8650(6)	12.9873(11)
Tl_9BiTe_6	830	980	8.8545(4)	13.0476(7)

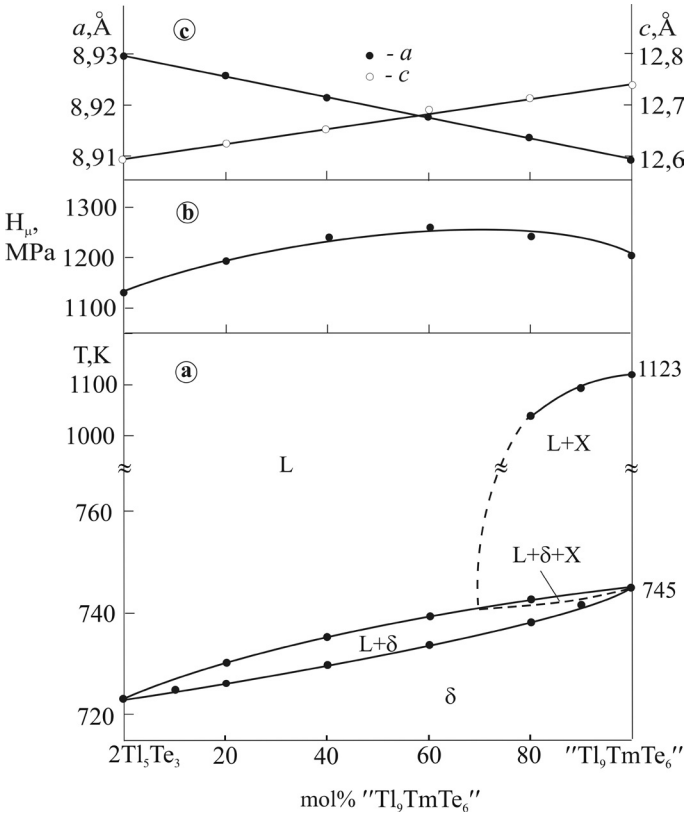

Figure 1. Phase diagram (a), concentration relations of microhardness (b), and lattice parameters (c) for the $2Tl_5Te_3$-Tl_9TmTe_6 section of the Tl-Bi-Tm-Te system.

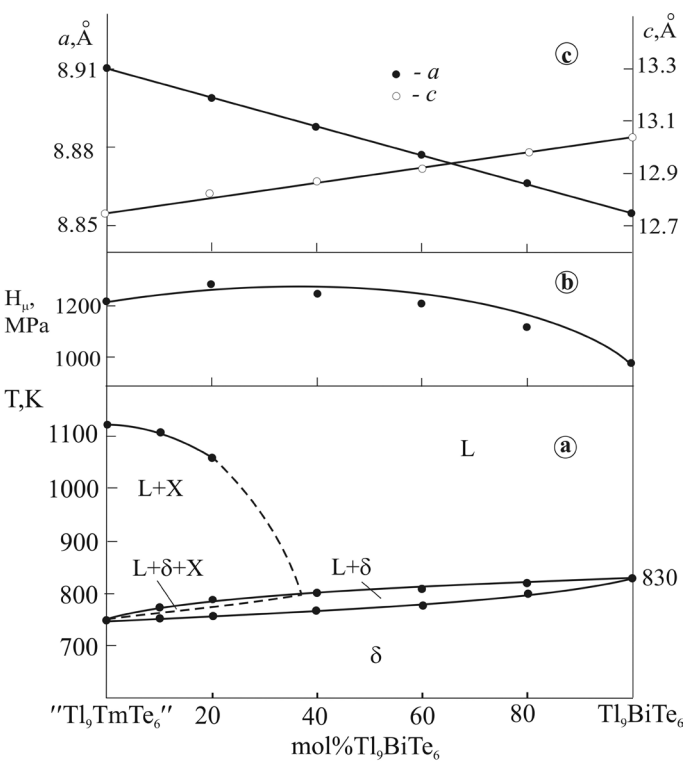

Figure 2. Phase diagram (a), concentration relations of microhardness (b), and lattice parameters (c) for the Tl_9TmTe_6-Tl_9BiTe_6 section of the Tl-Bi-Tm-Te system.

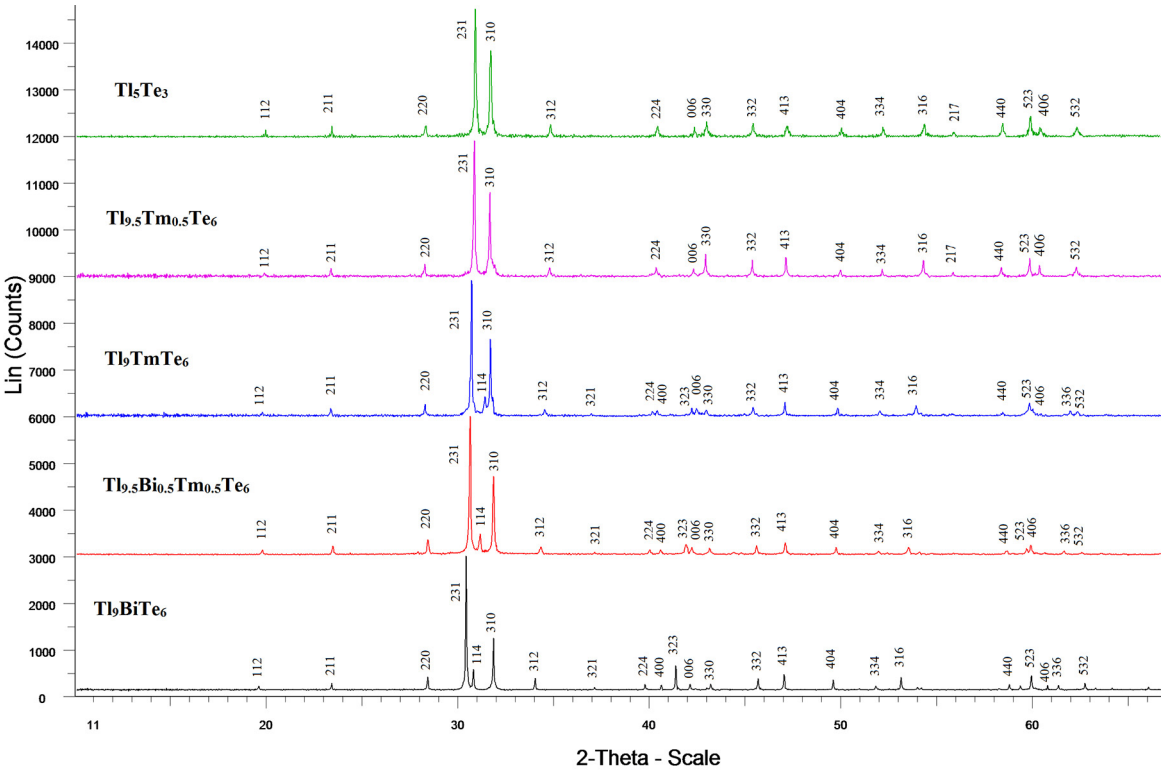

Figure 3. XRD patterns for some alloys of the Tl_5Te_3-Tl_9TmTe_6 and Tl_9TmTe_6-Tl_9BiTe_6 systems.

areas. The L+X+δ area is not fixed experimentally due to narrow temperature interval and shown by dotted line.

We have assumed that the X phase has a composition $TlTmTe_2$. This assumption is confirmed by the presence of the most intense reflection peaks of $TlTmTe_2$[28] on diffractograms of the as-cast alloys from region more than 63 mol% Tl_9TmTe_6.

Microhardness measurements (Figures 1b, 2b) are in good agreement with T-x phase diagram: curves have a flat maximum, which is typical for systems with continuous solid solutions.

Figure 3 presents the XRD patterns for some alloys of the Tl_5Te_3-Tl_9TmTe_6 and Tl_9TmTe_6-Tl_9BiTe_6 systems. As can be seen, powder diffraction patterns of starting compounds and intermediate alloys are single-phase and have the similar with Tl_5Te_3 diffraction pattern with slight reflections displacement from one composition to another. The lattice parameters of solid solutions obey the Vegard's law, i.e. depend linearly on composition (Table 1, Figures 1c, 2c).

Isopleth sections of the Tl_5Te_3-Tl_9BiTe_6-Tl_9TmTe_6 system (Figure 4).

Figures 4a-c show the isopleth sections Tl_9BiTe_6-[A], Tl_9TmTe_6-[B] and Tl_5Te_3-[C] of the Tl_5Te_3-Tl_9BiTe_6-Tl_9TmTe_6 system, where A, B and C are equimolar compositions of the boundary systems as shown in Figure 5a.

Over the entire compositions range of the Tl_9BiTe_6-[A] и Tl_5Te_3-[C] systems (Figures 4 a,c) only δ-phase crystallizes from the melt.

According to Figure 4a, along the Tl_9TmTe_6-[B] section in the composition area below 70 mol% Tl_9TmTe_6, the primary crystallization of the δ-phase occurs. In the Tl_9TmTe_6- rich interval the X-phase crystallizes first, followed by a monovariant peritectic process L+X↔δ.

The liquidus and solidus surfaces projections and isothermal section at 760 K in the Tl_5Te_3-Tl_9BiTe_6-Tl_9TmTe_6 composition area of the Tl-Bi-Tm-Te quaternary system (Figure 5).

Liquidus of Tl_5Te_3-Tl_9BiTe_6-Tl_9TmTe_6 section (Figure 5a) consists of two fields of the primary crystallization of X-phase and δ- solid solutions. These fields are separated by curve corresponding to the monovariant peritectic equilibrium L+X↔δ (ab curve). The solidus (dashed lines) consist of one surface of the completion of the crystallization of the δ-phase.

The isothermal section at 760 K is shown in Figure 5b. This section consists of five fields. In alloys containing < 65 mol% Tl_9TmTe_6 in the two-phase L+δ region the directions of the tie-lines are on the studied composition plane. Therefore, this part of the section can be considered stable. In the two-phase area L+X and also in the part of

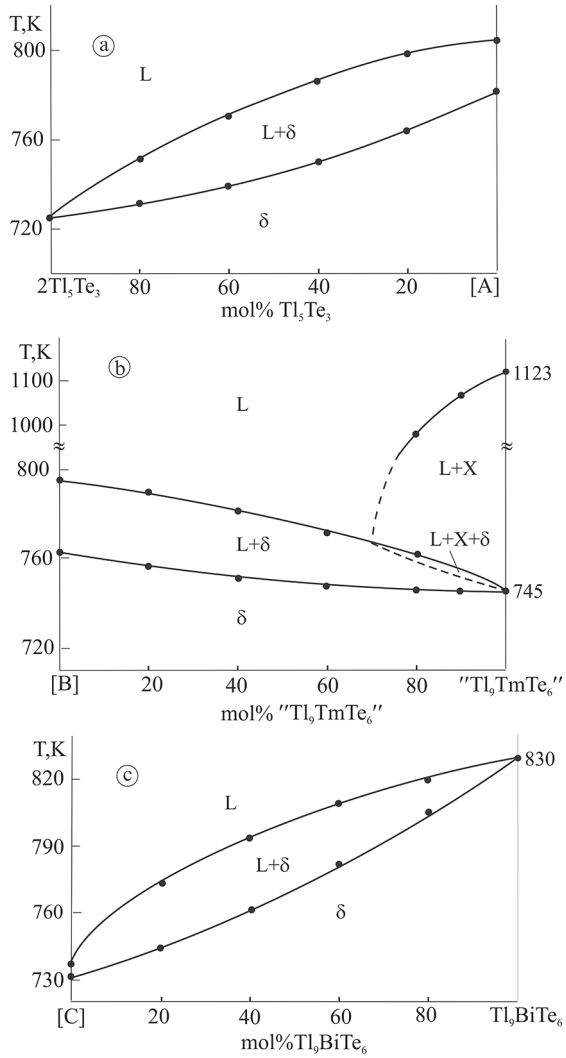

Figure 4. Polythermal sections $2Tl_5Te_3$-[A], Tl_9TmTe_6-[B] and Tl_9BiTe_6-[C] of the phase diagram of the Tl_5Te_3-Tl_9BiTe_6-Tl_9TmTe_6 section of the Tl-Bi-Tm-Te system. A, B and C are equimolar compositions of the boundary systems as shown in Fig.5a.

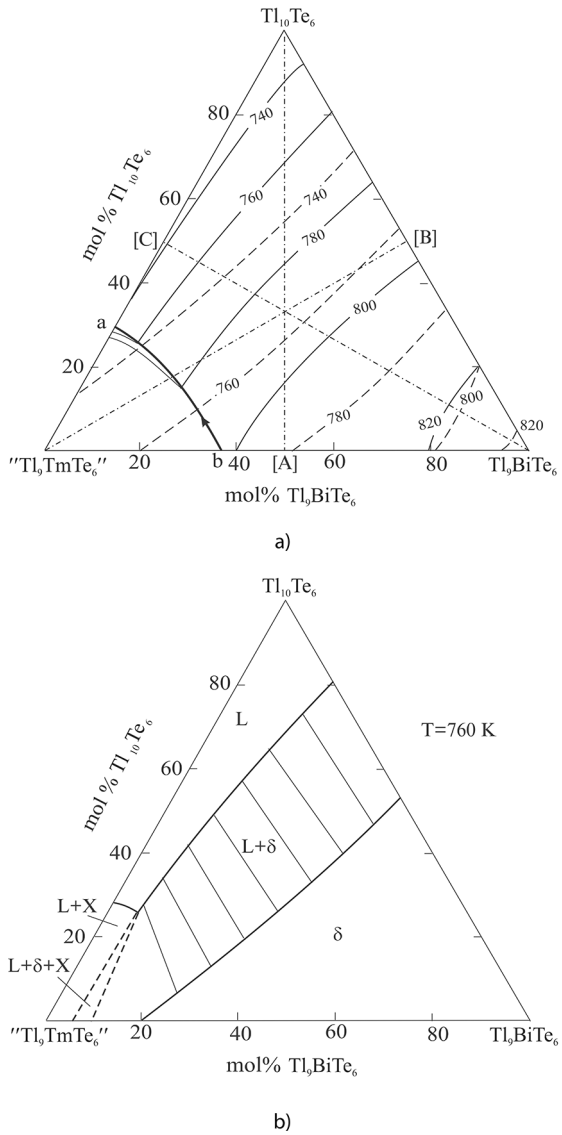

Figure 5. The liquidus and solidus surfaces projections and isothermal section at 760 K in the Tl_5Te_3-Tl_9BiTe_6-Tl_9TmTe_6 composition area of the Tl-Bi-Tm-Te quaternary system. Dash-dot lines show the investigated sections. A, B and C are equimolar compositions of the boundary systems.

L+δ area (Tl_9TmTe_6-rich composition) the directions of the tie-lines beyond the scope of this composition planes. Narrow three-phase L+X+δ region that must be between the above-pointed two-phase regions is not fixed and shown in Figure 5b by dotted line.

From Figure 5a it can be shown that the isothermal section at 780 K is qualitatively similar to one at 760 K (Figure 5b). Isothermal sections at 740, 800 and 820 K only consist of three fields of L-, X- and δ- phases.

It is worth noting that, comparison of the isothermal section (Figure 5b) and isopleth sections (Figure 4) shows that the directions of the tie-lines in the L+δ two-phase region deviate from the *T–x* plane and constantly vary with temperature.

4. Conclusion

The phase diagram of the Tl-Bi-Tm-Te system in the Tl_5Te_3-Tl_9BiTe_6-Tl_9TmTe_6 composition area is constructed, including the T-x diagrams of boundary systems Tl_5Te_3-Tl_9TmTe_6 and Tl_9BiTe_6-Tl_9TmTe_6, some isopleth sections, isothermal section at 760 K as well as the liquidus and solidus surfaces projections. The studied section is characterized by an unlimited solubility of components in the solid state. Obtained experimental data can be used for choosing the composition of solution-melt and determining the temperature conditions for growing crystals of δ- phase with a given composition.

5. Acknowledgment

The work has been carried out within the framework of the international joint research laboratory "Advanced Materials for Spintronics and Quantum Computing" (AMSQC) established between Institute of Catalysis and Inorganic Chemistry of ANAS (Azerbaijan) and Donostia International Physics Center (Basque Country, Spain).

6. References

1. Ahluwalia GD, ed. *Applications of Chalcogenides: S, Se, and Te*. Basel: Springer International Publishing; 2016.

2. Rowe DM, ed. *CRC Handbook of Thermoelectrics*. New York: CRC Press; 1995.

3. Jha AR. *Rare Earth Materials: Properties and Applications.* New York: CRC Press; 2014.

4. Yan B, Zhang HJ, Liu CX, Qi XL, Frauenheim T, Zhang SC. Theoretical prediction of topological insulator in ternary rare earth chalcogenides. *Physical Review B*. 2010;82(16):161108(R)-7.

5. Singh N, Schwingenschlögl U. $LaBiTe_3$: An unusual thermoelectric material. *Physica Status Solidi (RRL) - Rapid Research Letters*. 2014;8(9):805-808.

6. Wu F, Song H, Jia J, Hu X. Effects of Ce, Y, and Sm doping on the thermoelectric properties of Bi_2Te_3 alloy. *Progress in Natural Science: Materials International*. 2013;23(4):408-412.

7. Alemi A, Klein A, Meyer G, Dolatyari M, Babalou A. Synthesis of New $Ln_xBi_{2-x}Se_3$ (*Ln*: Sm^{3+}, Eu^{3+}, Gd^{3+}, Gd^{3+}) Nanomaterials and Investigation of Their Optical Properties. *Zeitschrift für anorganische und allgemeine Chemie*. 2011;637(1):87-93.

8. Schewe I, Böttcher P, von Schnering HG. The crystal structure of Tl_5Te_3 and its relationship to the Cr_5B_3 type. *Zeitschrift für Kristallographie*. 1989;188:287-298.

9. Babanly MB, Akhmadyar A, Kuliev AA. System Tl-Sb-Te. *Russian Journal of Inorganic Chemistry*. 1985;30(4):1051-1059.

10. Babanly MB, Akhmadyar A, Kuliev AA. System Tl_2Te-Bi_2Te_3-Te. *Russian Journal of Inorganic Chemistry*. 1985;30(9):2356-2359.

11. Gotuk AA, Babanly MB, Kuliev AA. Phase equilibria in the Tl-Sn-Te system. *Inorganic Materials*. 1979;15(8):1356-1361.

12. Wolfing B, Kloc C, Teubner J, Bucher E. High performance thermoelectric Tl_9BiTe_6 with an extremely low thermal conductivity. *Physical Review Letters*. 2001;86(19):4350-4353.

13. Arpino KE, Wallace DC, Nie YF, Birol T, King PDC, Chatterjee S, et al. Evidence for Topologically Protected Surface States and a Superconducting Phase in $[Tl_4]$ $(Tl_{1-x}Sn_x)Te_3$ Using Photoemission, Specific Heat, and Magnetization Measurements, and Density Functional Theory. *Physical Review Letters*. 2014;112:017002-5.

14. Imamalieva SZ, Sadygov FM, Babanly MB. New thallium neodymium tellurides. *Inorganic Materials*. 2008;44(9):935-938.

15. Babanly MB, Imamaliyeva SZ, Babanly DM, Sadygov FM. Tl_9LnTe_6 (Ln-Ce, Sm, Gd) compounds – new structural analogies of Tl_5Te_3. *Azerbaijan Chemical Journal*. 2009;2:121-125. (in Russian).

16. Babanly MB, Imamaliyeva SZ, Sadygov FM. Physico-chemical interaction of Tl and Tm (Yb) tellurides. *Baku University News. Series of Nature Study*. 2009;4:5-10. (in Russian).

17. Imamalieva SZ, Mashadiyeva LF, Zlomanov VP, Babanly MB. Phase equilibria in the Tl_2Te-YbTe-Te system. *Inorganic Materials*. 2015;51(11):1237-1242.

18. Bangarigadu-Sanasy S, Sankar CR, Schlender P, Kleinke H. Thermoelectric properties of $Tl_{10-x}Ln_xTe_6$, with Ln = Ce, Pr, Nd, Sm, Gd, |Tb, Dy, Ho and Er, and $0.25 \leq x \leq 1.32$. *Journal of Alloys and Compounds*. 2013;549:126-134.

19. Bangarigadu-Sanasy S, Sankar CR, Dube PA, Greedan JE, Kleinke H. Magnetic properties of Tl_9LnTe_6, Ln = Ce, Pr, Gd and Sm. *Journal of Alloys and Compounds*. 2014;589:389-392.

20. Guo Q, Kleinke H. Thermoelectric properties of hot-pressed Tl_9LnTe_6 (Ln = La, Ce, Pr, Nd, Sm, Gd, Tb) and $Tl_{10-x}La_xTe_6$ $(0.90 \leq x \leq 1.05)$. *Journal of Alloys and Compounds*. 2015;630:37-42.

21. Ioffe AF. *Semiconductor Thermoelements and Thermoelectric Cooling*. London: Infosearch; 1957.

22. Babanly MB, Tedenac JC, Imamalieva SZ, Guseynov FN, Dashdieva GB. Phase equilibria study in systems Tl-Pb(Nd)-Bi-Te new phases of variable composition on the base of Tl_9BiTe_6. *Journal of Alloys and Compounds*. 2010;491(1-2):230-236.

23. Imamaliyeva SZ, Guseynov FN, Babanly MB. Phase diagram of Tl_5Te_3-Tl_4PbTe_3-Tl_9NdTe_6 system and some properties of solid solutions. *Chemical Problems*. 2008;4:640-646. (in Russian).

24. Imamaliyeva SZ, Guseynov FN, Babanly MB. Phase equilibria and properties of solid solutions in the system Tl_9NdTe_6-Tl_9BiTe_6-Tl_4PbTe_3. *Azerbaijan Chemical Journal*. 2009;1:49-53. (in Russian).

25. Asadov MM, Babanly MB, Kuliev AA. Phase equilibria in the Tl-Te system. *Inorganic Materials*. 1977;13(8):1407-1410.

26. Imamaliyeva SZ. T-x diagram of the Tl_2Te-Tl_9TmTe_6 system. *International Journal of Applied and Fundamental Research*. 2016;6(3):451-455.

27. Doert T, Böttcher P. Crystal structure of bismuth nonathallium hexatelluride $BiTl_9Te_6$. *Zeitschrift für Kristallographie*. 1994;209(1):95.

28. Duczmal M, Pawlak L. Magnetic properties and crystal field effects in $TlLnX_2$ compounds (X = S, Se, Te). *Journal of Alloys and Compounds*. 1997;262-263:316-319.